

Nanoscale Automated Phase and Orientation Mapping in the TEM

A. D. Darbal,^{1,2} * M. Gemmi,³ J. Portillo,^{1,4} E. Rauch,⁵ and S. Nicolopoulos¹

¹ NanoMEGAS SPRL, Blvd Edmond Machtens 79, B-1080 Brussels, Belgium

² AppFive LLC, 1095 W. Rio Salado Suite 110, Tempe, AZ 85281

³ Center for Nanotechnology Innovation@NEST, Italian Institute of Technology, Piazza San Silvestro 12, Pisa, Italy

⁴ Ccit University of Barcelona, c/Sole i Sabaris, 08028 Barcelona, Spain

⁵ Laboratoire SIMaP, Grenoble INP – CNRS - UJF, BP 46 - 38402 Saint Martin d'Hères Cedex, France

*amith@appfive.com

Editor's Note: *This article describes a method that received the Microscopy Today Innovation Award in 2011.*

Introduction

The limitation of spatial resolution in orientation imaging via electron backscattered diffraction analysis in the scanning electron microscope (SEM) makes it difficult to investigate the microstructure of nanocrystalline materials. The use of the recently developed transmission electron microscope (TEM) based product, known as ASTAR, offers the possibility of reliable orientation/phase mapping with a spatial resolution below 3 nm. In ASTAR, a nanoprobe electron beam is scanned over the specimen, and spot diffraction patterns are collected. The electron beam is precessed to reduce dynamical effects and improve pattern quality. Using template matching, the diffraction patterns are indexed automatically.

The most widely used approach to quantify microstructure and microtexture is through the determination of crystal orientation by the analysis of electron back-scattered diffraction (EBSD) patterns in a SEM [1]. The analysis of EBSD patterns in SEM has reached a high degree of automation, and it is now possible to determine the crystal orientation from each point of the scanned area. This is commonly referred to as orientation microscopy (OM). However, the use of SEM-EBSD analysis for OM has certain limitations. The most important of which being that its spatial resolution is limited to approximately 50 nm [2]. Furthermore it is difficult to obtain clear EBSD patterns from heavily deformed materials, and a pristine specimen surface is a pre-requisite for obtaining reliable maps using EBSD in the SEM.

Given the ever-increasing application of nanocrystalline (average grain size < 100 nm) materials in modern technology, there is a need for microstructure characterization tools with high spatial resolution. This has motivated the development of OM in the TEM, which can, in principle, provide an order of magnitude improvement in the spatial resolution compared to SEM-EBSD analysis. Several approaches toward OM using diffraction methods in the TEM have been explored. These include the automated analysis of convergent beam diffraction patterns, transmission Kikuchi patterns, and diffraction patterns reconstructed using dark field images. The interested reader is referred to an in-depth review of all the OM techniques [3]. Even though these methods offer, in principle, high-spatial resolution, there are limitations that make these approaches unsuitable in many cases. The presence of strong dynamical effects in electron diffraction is a serious limitation in many situations as the kinematical theory is no

longer applicable, leading to unreliable orientation solutions. Inadequate sampling of higher-order reflections is another limitation, especially with reconstructed diffraction patterns.

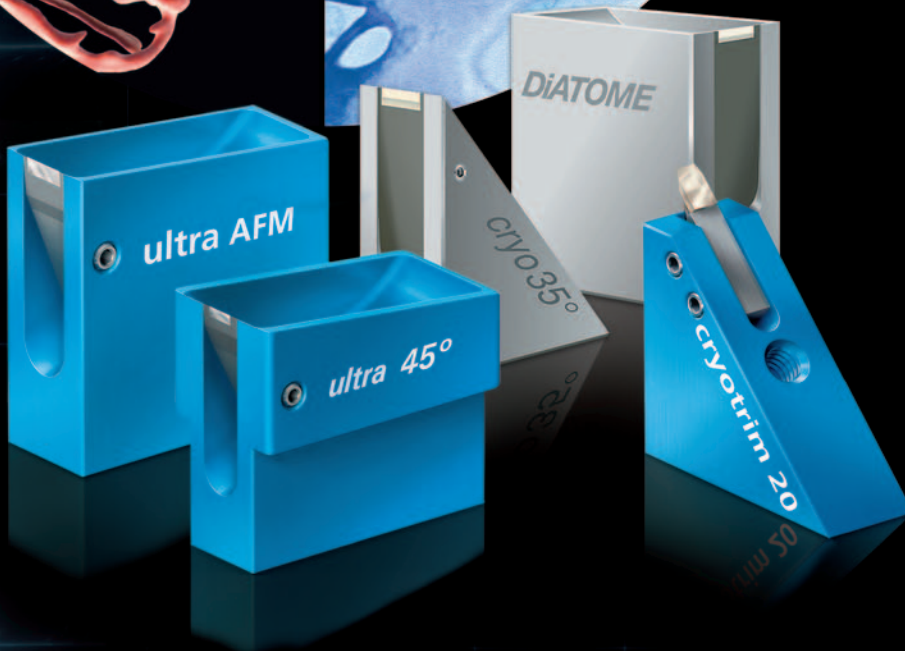
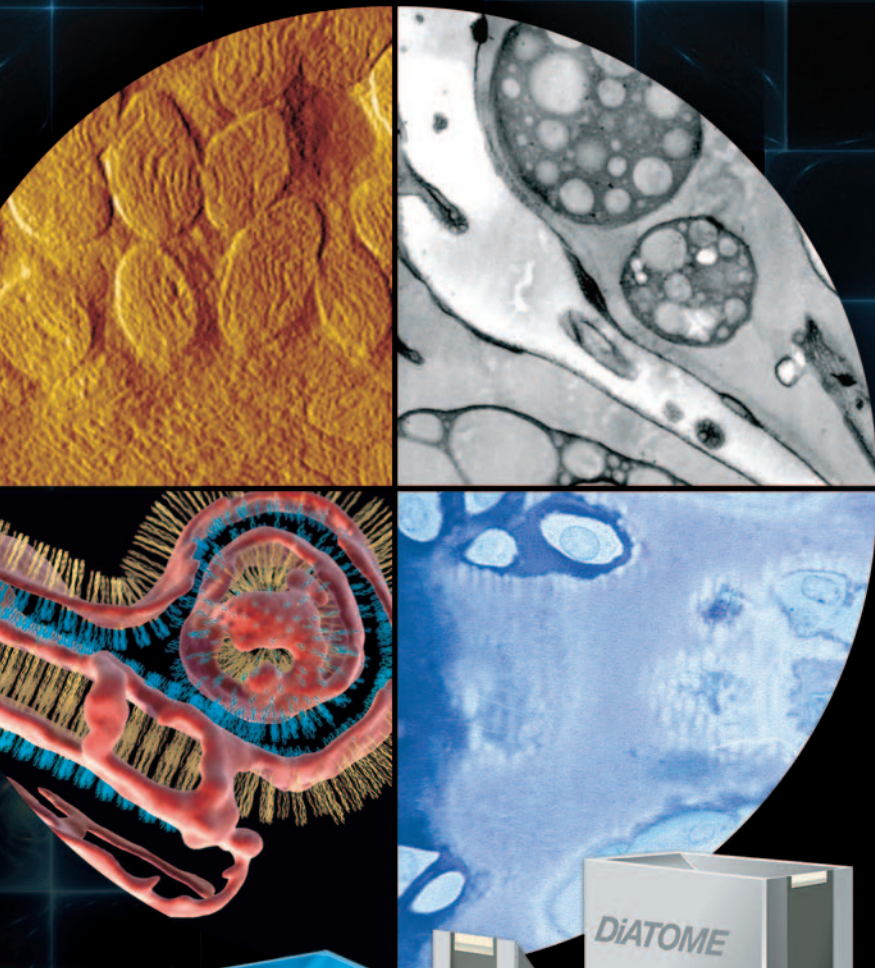
In a more recent advancement, automated indexing of spot diffraction patterns acquired by scanning a quasi-parallel nanobeam has been employed for OM in the TEM [4]. Several reports show the success of this approach toward acquiring reliable orientation maps. Further improvement in this approach has been achieved by precessing the beam as it is scanned to reduce the strong dynamical effects and by better sampling of spots in a higher-order Laue zone (HOLZ). This is the basis of the ASTAR system, manufactured by NanoMEGAS, for automated orientation imaging and phase mapping in the TEM [5]. In the following sections of this article, we discuss the ASTAR system in more detail. The principle of precession microscopy and its importance in electron diffraction analysis is described. Examples are presented to show the applications of ASTAR-generated orientation and phase maps from materials of technological and scientific interest.

Precession Microscopy

The presence of strong dynamical interactions and the difficulty of recording sufficient higher-order reflections is a severe limitation for quantitative investigation using electron diffraction. This problem has been tackled in X-ray diffraction by rocking the crystal, thereby integrating intensities over a range of crystal orientations. However, a similar approach in a TEM would limit the spatial resolution to a few micrometers because of machining tolerances in the mechanical drives used to rock the specimen. An alternative approach is to precess the electron beam, which is formally equivalent to rocking the specimen.

The use of precession in electron diffraction was introduced by Vincent and Midgley [6]. In precession electron diffraction (PED), the incident beam is double-deflected in a conical scan and the diffraction intensities are integrated over the entire scan (Figure 1a). As the incident beam undergoes precession, the diffraction pattern moves on the screen. To compensate for the movement of the diffraction pattern, after the specimen the beam is tilted in a complementary way so that the diffraction pattern remains stationary on the screen. Precession diffraction is used to achieve quasi-kinematical conditions. Dynamical effects are reduced as the incident beam is not exactly on axis and fewer beams are excited simultaneously. The use of precession also enables the collection of a higher number of reflections, including reflections

**the highest quality...
the most precise sectioning...
incomparable durability**



Free Customer Service

Sectioning tests with biological and material research specimens of all kinds. We send you the sections along with the surfaced sample, a report on the results obtained and a recommendation of a suitable knife. Complete discretion when working with proprietary samples.

Re-sharpening and Reworking Service

A re-sharpened Diatome diamond knife demonstrates the same high quality as a new knife. Even knives purchased in previous years can continue to be re-sharpened. The knives can be reworked into another type of knife for no extra charge, e.g. ultra to cryo or 45° to 35°.

Exchange Service

Whenever you exchange a knife we offer you a new Diatome knife at an advantageous price.

40 years of development,
manufacturing, and
customer service

DiATOME
diamond knives

ultra 45° • cryo • histo • ultra 35° • STATIC LINE II
cryo-P • cryo immuno • ultra sonic
cryotrim 45 and 25 ultra • AFM & cryo AFM • cryo 25°

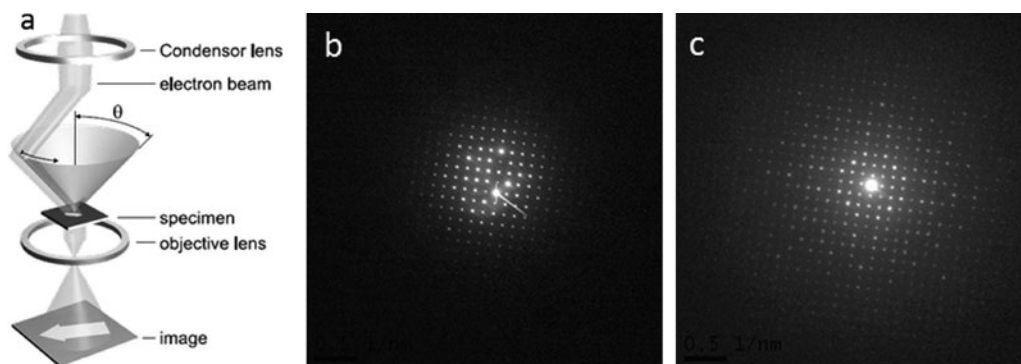


Figure 1: (a) Precessed illumination of the sample. Examples of a diffraction pattern (b) without precession and (c) with 2.5° precession taken on a cubic mayenite crystal.

from HOLZs, which is useful in eliminating the ambiguities in indexing the spot diffraction patterns. Additionally, it is possible to obtain quite symmetric patterns even when the crystal is off the zone axis when precession is employed. The improvement in the quality of spot patterns with precession can be seen by comparing the two diffraction patterns shown in Figures 1b and 1c. The use of PED patterns is, therefore, a significant improvement over using conventional spot patterns for orientation and phase identification. In addition, precession-assisted spot patterns are less sensitive than EBSD patterns to the crystal deformation state, grain size, and foil thickness. In many cases, PED patterns reduce the risk of incorrect interpretation.

DigiSTAR, part of the ASTAR hardware, is a digital precession instrument developed by NanoMEGAS. DigiSTAR is connected to the TEM beam and image deflector coils and can be retrofitted into old TEMs or mounted onto new ones. Using DigiSTAR, it is possible to drive the beam and image deflector coils simultaneously to achieve different precession frequencies and angles. Furthermore, because the alignment values to drive the deflector coils are stored digitally, the same DigiSTAR hardware can be used for precession on more than one TEM.

ASTAR Setup and Operation

A schematic diagram of the setup for the ASTAR system is shown in Figure 2. In ASTAR, spot diffraction patterns are acquired sequentially using a high-speed optical CCD camera

while an area on the sample is being scanned by a nano-sized quasi parallel probe. At the same time the incident beam is precessed about the optic axis. Precession and beam scanning are controlled by an electronics unit that allows control of beam pivot points and descanned pivot points. The camera, with an 8-bit dynamic range, is mounted in front of the TEM fluorescent screen and captures the diffraction patterns projected on the fluorescent screen. The camera can capture images up to 180 frames per second, which is crucial for a high acquisition speed. The ASTAR hardware unit can be retrofitted into modern TEMs and does not require the TEM to have its own beam-scanning unit.

As the beam is scanned over a pre-selected specimen area, a spot diffraction pattern from each step in the scan is recorded and stored in a dedicated computer. Using the kinematical theory of diffraction, spot diffraction patterns corresponding to all possible orientations for all are calculated. If more than one phase is present, then diffraction patterns corresponding to all possible orientations for each of the phases present is calculated. A stack of all possible diffraction patterns generated is known as a template bank. It should be noted that the crystallographic structure of all the phases present should already be known to generate the template bank. Every experimental diffraction pattern is then compared using cross-correlation with each of the pre-calculated patterns in the template bank. The degree to which a pre-calculated pattern matches the experimental pattern is given by the correlation index. A higher correlation index implies a better matching solution. The pattern with the highest correlation index, therefore, gives both the orientation and phase solution. Figure 2c shows the essence of the matching process using cross-correlation. The pattern (in red) overlaid on top of the experimental pattern has the highest correlation index compared to all other patterns in the template bank. Figure 2d shows the correlation index, on a gray scale intensity plot, corresponding to all possible

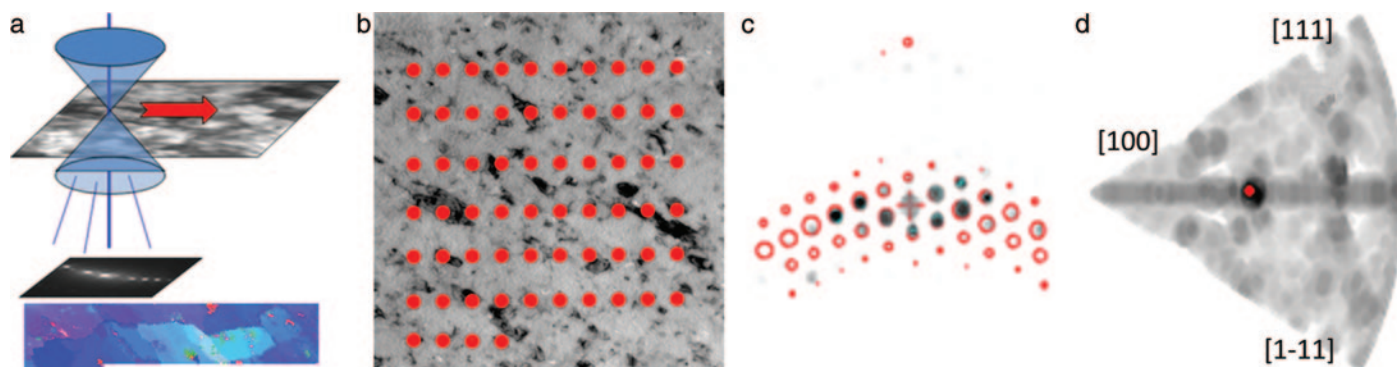


Figure 2: Precession-assisted orientation mapping: (a–b) beam-scanning over a user-defined sample area coupled with precession, (c), superposition of the best matching template (red dot pattern) with the experimental pattern (gray dot pattern), and (d) correlation index values on a gray scale intensity plot corresponding to each of the orientations possible where the crystal orientations are represented on a stereographic projection. Darker regions correspond to a higher correlation index.

orientations for the given crystal symmetry represented on a stereographic projection. The orientation corresponding to the red dot in Figure 2d has the highest correlation index.

A typical acquisition time for a scan area of 500×500 pixels is approximately 20 minutes (200 points per second). The analysis of the acquired diffraction patterns can be done offline and takes about 5 minutes for highly symmetrical cubic materials. Typically, around 2000 templates are generated, which provides approximately 1° angular resolution.

The ASTAR system allows the user to generate a virtual bright-field image, a correlation index, and a reliability map, corresponding to a given orientation map [4]. These maps serve as a useful reference and provide a means to evaluate the “goodness” of the orientation maps. A virtual bright-field image is generated by plotting the intensity variation of the transmitted beam in the stack of diffraction patterns as a function of the pixel coordinates in the scan area. A correlation index map is generated by plotting the value of the correlation index for the best matching template to each diffraction pattern. An example of a correlation index map is shown in Figure 3b, where the region in black has a low correlation index. The correlation index is very useful in identifying the crystalline region of interest from the surrounding amorphous regions. For non-crystalline regions, the diffraction pattern contains only the transmitted beam but does not show any Bragg diffraction spots. Therefore, the correlation index value is much lower than it is for crystalline regions. The reliability index, analogous to the SEM-EBSD confidence index, is given by the ratio of correlation index for the best matching and the second-best matching templates. It is defined in a way such that the reliability index is zero when more than one solution is possible for the diffraction pattern. A reliability map is a gray scale intensity plot of reliability index values for each pixel in the scan area. The reliability map is particularly useful in identifying grain boundaries as the grain boundaries have low reliability values. At grain boundaries, the diffraction pattern is an overlap of patterns arising from the overlapping crystals meeting at the grain boundary. Therefore, there is more than one solution possible and, consequently, low reliability at grain boundaries.

Application Examples

This section demonstrates some applications of PED for microstructural analysis in materials science. The first example shows an orientation map from Pt nanocrystals along with the correlation index map (Figure 3). 1 nm spatial resolution for orientation maps of nanocrystals can be obtained with a FEG-TEM microscope [7]. The surrounding amorphous regions can be distinguished from the Pt crystals using the correlation index map (Figure 3b).

Figure 4 shows the application of PED orientation

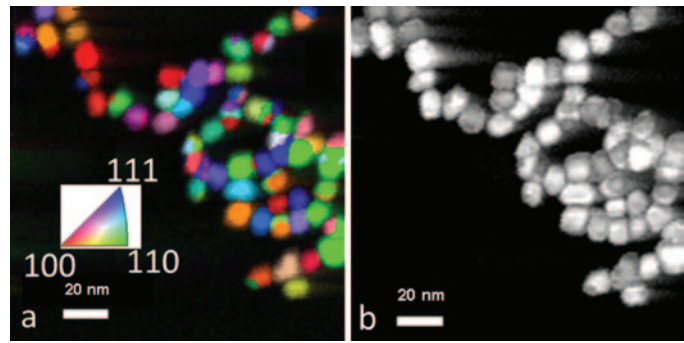


Figure 3: Platinum nanocrystal. (a) Orientation map of nanocrystals. The orientation map shows the orientation of the sample normal in the crystal reference frame according to the color code shown in the inset. The same color-coding is used for all of the orientation maps in this article. (b) Correlation index map. The dark regions in the orientation and correlation index map are the amorphous regions. A precession angle of 0.5° was used, and the microscopy was performed on a JEOL 2010 FEG TEM. Courtesy of Prof. P. Ferreira and Dr. K. J. Ganesh, Univ of Texas at Austin.

mapping to the study of a heavily deformed Fe [8]. The aim of this study was to investigate the microstructural evolution of high-purity Fe samples with severe plastic deformation. It was found that the deformation leads to a continuous misorientation gradient within the grains, with no sub-grain formation detected [8]. In Figure 4, the reliability map is overlaid on the orientation map so that the intensity variation in the orientation map corresponds to the variation in the reliability index. The dark regions in the orientation map correspond to grain boundaries, which have low reliability index.

Figure 5 shows an example of phase identification using ASTAR software in a heavily deformed Fe-14Cr-16Ni steel specimen. The phase map (Figure 5b) shows the presence of a small fraction of martensite at the triple junctions. The bright-field image (Figure 5a) from the same specimen area shows the difficulty in accurately identifying phases using conventional imaging techniques.

Nanotechnology is another possible field where PED can obtain interesting results. Figure 6 shows the phase and

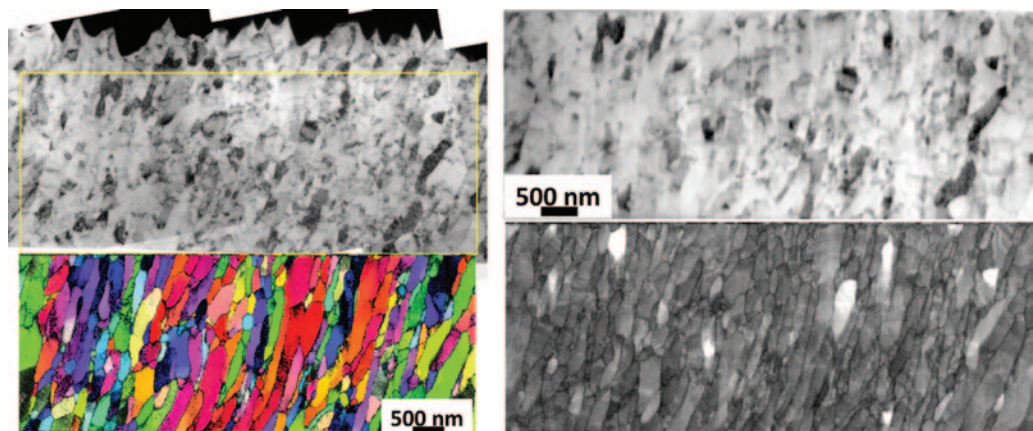


Figure 4: Orientation mapping of severely deformed iron. Image at the (upper left) shows the region of the thin foil examined. Orientation map is combined with the reliability map to highlight grain boundaries (lower left) so that the dark regions correspond to regions with low reliability index values. Note that grains are hardly noticed on the bright-field image of the same area (upper right). The exact scanned area can be identified with the help of the virtual bright-field image (upper right) that is constructed with the same set of data as orientation, reliability, and matching index (lower right). See reference [8] for details. Microscopy was performed on a JEOL 3010 LaB₆ TEM.

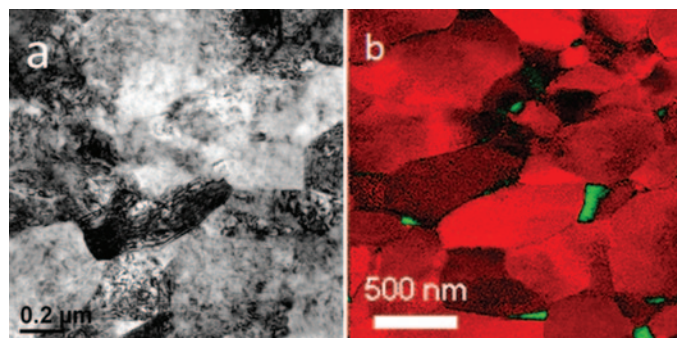


Figure 5: (a) Representative TEM bright-field image and (b) the phase map from an austenitic steel sample. Small fraction of martensite (green) was observed at the triple junctions. Sample courtesy of Prof. Yong, Univ. of Central Florida. Microscopy was performed on a JEOL 2010 FEG TEM operating at 200 kV.

orientation mapping of a $\text{InAs}/\text{InAs}_x\text{Sb}_{1-x}/\text{InAs}$ heterostructured nanowire (NW) [9]. The InAs NWs have a hexagonal wurzite structure. However, by addition of Sb to form a ternary alloy, the wire changes to a cubic zinc blende structure. The PED orientation maps identify the $\text{InAs}_x\text{Sb}_{1-x}$ cubic sector of the InAs NW and further reveal that the cubic structure of the alloy transforms back into the hexagonal InAs with a twinned layer of approximately 30 nm in thickness.

Conclusion

The ASTAR system is an orientation and phase mapping tool for the TEM combining the acquisition of electron diffraction spot patterns, pattern matching techniques, and precession microscopy. The use of a high-frame-rate camera ensures rapid acquisition, thereby making it possible to obtain large orientation data sets. The use of precession to improve diffraction pattern quality is another significant advantage. The spatial resolution offered by this technique is a significant improvement over SEM-EBSD analysis because orientation/phase mapping can be obtained with a spatial resolution of 1–5 nm with FEG-TEMs. Samples from metals to mineral and from semiconductors to nanoparticles can be studied with any TEM using standard specimen preparation techniques.

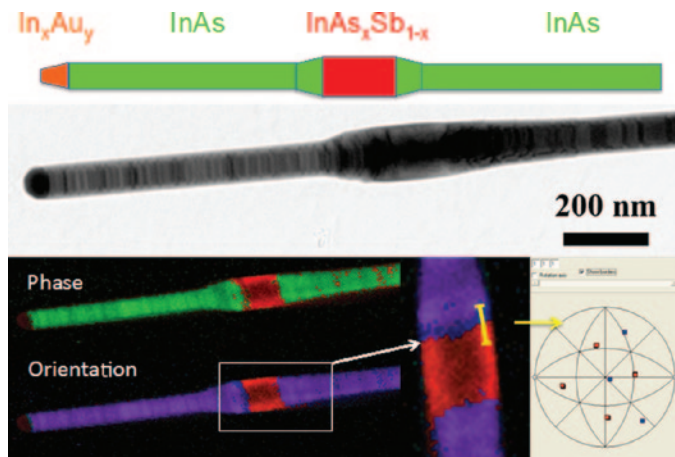


Figure 6: (Top) Sketch of a $\text{InAs}/\text{InAs}_x\text{Sb}_{1-x}/\text{InAs}$ heterostructured nanowire (NW) and TEM bright-field image of one NW. (Bottom) Corresponding phase (green: hexagonal wurzite; red: cubic zinc blende) and orientation mapping. In the bottom image, the magnified image of the $\text{InAs}_x\text{Sb}_{1-x}$ sector (inset), it is possible to identify a 30 nm twinned layer of cubic zinc blende (blue part) structure at the boundary with the top InAs wire. A stereographic projection of the [111] directions along the yellow line is displayed at the right. The data were collected on a Zeiss Libra 120. Courtesy of Lucia Sorba CNR-Istituto Nanoscienze and Daniele Ercolani NEST Scuola Normale Superiore, Pisa, Italy.

References

- [1] D Dingley, *J Microsc-Oxford* 213 (2004) 214–24.
- [2] S Zaeferrer, *J Appl Crystallogr* 33 (2000) 10–25.
- [3] S Zaeferrer, *Cryst Res Technol* 46 (2011) 607–28.
- [4] EF Rauch and L Dupuy, *Archives of Metallurgy and Materials* 50 (2005) 87–89.
- [5] J Portillo, EF Rauch, S Nicolopoulos, M Gemmi, and D Bultreys, *Mater Sci Forum* 644 (2010) 1–7.
- [6] R Vincent and PA Midgley, *Ultramicroscopy* 53 (1994) 271–82.
- [7] KJ Ganesh, M Kawasaki, JP Zhou, and PJ Ferreira, *Microsc Microanal* 16 (2010) 614–21.
- [8] S Descartes, C Desrayaud, and EF Rauch, *Mater Sci Eng A* 528 (2011) 3666–75.
- [9] D Ercolani, M Gemmi, L Nasi, F Rossi, M Pea, A Li, G Salviati, F Beltram, and L Sorba, *Nanotechnology* 23 (2012) 115606.

MT

SEM Digi-Cam 3 Upgrade ANY Analog SEM



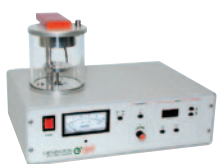
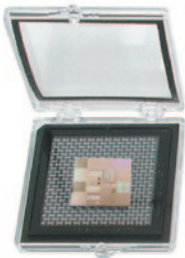
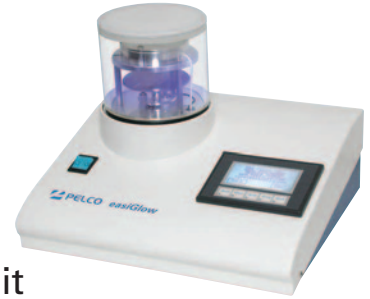
- ▶ Replaces Polaroid Film
- ▶ 14.1 MP Resolution
- ▶ X-Y-Z Adjustments
- ▶ Custom Made for any SEM
- ▶ Wireless Image Transfer
- ▶ Remote-Controlled Shutter Operation
- ▶ Basic Package \$3995 or \$4495 with PC
- ▶ 2–4 Weeks Delivery



www.semsupplies.com M.E. Taylor Engineering, Inc.
(301) 975-9798

Preparation Equipment and Microscopy Supplies

The single source for All your microscopy supplies and specimen preparation equipment.



- Vacuum Coating Systems
- Calibration Standards
- PELCO® easiGlow™ Glow Discharge Unit
- SEM Sample Holders and Mounts
- Silicon Nitride TEM Membranes
- PELCO BioWave Pro® Tissue Processor
- TEM Support Films
- AFM Supplies
- Quality Laboratory Tweezers
- Vacuum Pick-up Systems
- Digital Stereo Microscopes
- Conductive Adhesives
- FIB Supplies

Complete line of compact Cressington EM Sample Coaters.

